Please note that the Reviewer Comments are posted in Black, Author Responses posted in Red, and our proposed Revisions to the text posted in Blue.

- **The manuscript is presenting reconstructions of the northern sector of the former Patagonian ice sheet during the last glacial maximum (LGM) and subsequent deglaciation based on an ice sheet model ensemble driven by the climate model forcing from the PMIP4 and TRACE-21ka experiments. One shortcoming of this manuscript is an obvious disconnect between the LGM and deglaciation experiments – it almost feels like they belong to two separate studies. If this manuscript is to be published, the synergy between these two parts of the study must be improved considerably. There are also several issues with the methodology that adapts poorly justified assumptions and simplifications requiring much more detailed considerations and sensitivity tests. Finally, the interpretation of the large-scale processes driving regional climate changes is weak, and the link between climate models and paleoclimate proxy data is non-existent. Below I provide detailed instructions for major revisions of the study's design and contents that are required to merit a publication in TC.**

We would like to thank the reviewer for their consideration and generous suggestions as to improve the analysis and conclusions expressed in this paper. When considering their comments, we have decided to make some changes to our analysis. Based on new work that is in discussion at Climates of the Past (https://cp.copernicus.org/preprints/cp-2023-47/) which takes a deeper look into the PMIP4 climatologies and simulated LGM PIS behavior (in addition to Yan et al., 2020), we have, based upon the reviewer suggestions, to remove the PMIP analysis from this paper. Instead, and upon further analysis suggested by the reviewer, we have decided to focus on the LGM and last deglaciation simulations using TraCE-21ka climate forcings. To assess the role of the SWW and the influence of precipitation, we have performed two additional transient ice sheet simulations across the last deglaciation – see response to Reviewer Comment 3G below. We find that these new simulations provide stronger support to our initial conclusions regarding the modulating role precipitation may have played on influencing the pace and magnitude of deglaciation across our model domain.

We also thank the reviewer for the gentle nudge to look deeper into the deglacial climate changes simulated within the TraCE-21ka climate model. Below we highlight additional analysis of the TraCE-21ka model outputs across South America and our model domain. This analysis shows that TrACE-21ka simulates changes in the SWW position and strength, and ultimately the hydrologic cycle during the LGM and last deglaciation across the CLD. Additionally, we find that the TraCE-21ka simulated deglacial changes in precipitation and SWW qualitatively agree well with paleoclimate proxies of precipitation across the CLD, from which prior worked has used to infer deglacial changes in the SWW. We link this discussion to our ice sheet model results and provide more detailed commentary comparing simulated changes in TrACE-21ka precipitation and temperature to proxy records across the Chilean Lakes District that constrain deglacial climate change. From this analysis, we hope it is more clear that TraCE-21ka compares well against regional proxies of past climate change across the CLD, giving confidence that our ice sheet modelling is capturing changes consistent with the prevailing understanding of deglacial climate change in this region.

We respond to the other points raised by the reviewer by offering results of additional modelling experiments and clarifying our text to meet the reviewers' comments.

Major points:

- **Disconnect between two parts of the study: Both the results and discussion sections (especially the latter) have very weak links between the LGM and deglaciation components of the study. It is unclear why there is a need for the PMIP4-driven LGM experiments if they don't contribute much to the design of the transient simulations. More effort needs to be invested into strengthening the synergy through cross-model experiments and large-scale mechanism interpretation.**

- **2. Weak interpretation of the large-scale mechanisms:**
- **2a) The interpretation of the origins of temperature and precipitation anomalies and their impacts on the ice sheet formation and growth is weak. There are a lot of mentions of the southern westerly wind (SWW) system as a potential driver and yet no attempt to look into the climate model outputs and establish to which extent this process is a factor. The statements in the manuscript that paleoclimate proxies provide a confusing picture are not helpful and hint at an energy-saving mode of the study (minimum effort). Having global climate model outputs at hand, the authors need to step up and dive into the simulated climate dynamics and large-scale drivers of the inferred anomalies.**

Thank you for the push to look closer at local paleoclimate proxies of climate change across the CLD. We have bolstered the review of current literature surrounding paleoclimate change across the CLD, and the nature of how the SWW is interpreted to have changed based upon these proxy records. We have made changes to our introductory text and the discussion. In the discussion section we include more information that provides a qualitative comparison between TraCE-21ka simulated temperature and precipitation change across the CLD and information derived from proxies (e.g. vegetation, pollen).

We kindly push back on what the reviewer stated regarding, "The statements in the manuscript that paleoclimate proxies provide a confusing picture are not helpful and hint at an energy-saving mode of the study (minimum effort)." We would like to clarify that we never mentioned the paleo proxies being "confusing," nor was that our intention. We apologize for any miscommunication on our part.

Instead, we merely cited evidence from the literature to support the notion that it is very difficult to constrain SWW changes directly from paleo-proxy data. Perhaps this is best summarized in Kohfeld et al., 2013 who looked at a large dataset of paleoclimate proxies across the Southern Hemisphere (many over S. America) and concluded: "A chain of assumptions are needed to interpret paleodata as changes in the westerly wind position and intensity. Importantly, the modern relationships between Southern Hemisphere westerly winds and moisture must hold for past time periods, and over an increased latitudinal range at the LGM, compared with the present day…..These inherent assumptions, and the possibility for multiple interpretations of the observations, create uncertainty in conclusions regarding past changes in winds interpreted solely from data."

This is also supported by additional climate modelling work from Sime et al., 2013, whom Kohfeld state: "Combining these data compilations with model simulations is one approach for better understanding the role of winds in controlling glacial interglacial conditions. Sime et al. (2013) use this moisture reconstruction to assess impacts of LGM wind fields on moisture patterns from several AGCM and AOGCM simulations. Their results suggest that model simulations do a reasonable job of reproducing LGM moisture patterns without large shifts in glacial winds and provide one example of integrating model simulations with data compilations to understand ocean-atmosphere changes during the LGM."

Therefore, we have reworked our introduction and discussion to clarify any misunderstanding we may have created with our assessment.

<u>Introduction (Lines 71: 93), we have updated and added text accordingly:</u>

"Terrestrial paleoclimate proxies indicate that the CLD was wetter during the LGM and early deglaciation, supporting the idea that the SWW migrated northward of 41°S across the CLD (Moreno et al., 1999; Moreno et al., 2015; Moreno and Videla, 2016). Additionally, these proxies indicate a switch from hyperhumid to humid conditions around 17,300 cal yr BP, which was inferred by Moreno et al. (2015) to indicate the poleward migration of the SWW south of the CLD.

However, we note that inferring changes in the SWW across the last deglaciation from paleoclimate proxies can be problematic as outlined by Kohfeld et al. (2013) who compile an extensive dataset of proxy records that record changes in moisture, precipitation-evaporation balance, ice accumulation, runoff and precipitation, dust deposition, and marine indicators of sea surface temperature, ocean fronts, and biologic productivity across the Southern hemisphere. Kohfeld et al. (2013) conclude that environmental changes inferred from existing paleoclimate data could be potentially explained by a range of plausible scenarios for the state and change of the SWW during the LGM and last deglaciation, such as a strengthening, poleward or equatorward migration, or no change in the SWW. Climate model results from Sime et al. (2013) indicate that the reconstructed changes in moisture from Kohfeld et al. (2013) can be simulated well without invoking large shifts or changes in strength to the SWW. This discrepancy also exists amongst climate models which diverge on whether the LGM SWW was shifted equatorward or poleward, and was stronger or weaker (Togweiler et al., 2006; Menviel et al., 2008; Rojas et al., 2009; Rojas et al., 2013; Sime et al., 2013; Jiang et al., 2020). Therefore, from paleoclimate proxies and climate models, we still do not have a firm understanding of how the SWW may have changed during the last deglaciation, however, climate proxies and models can still be effectively used to evaluate regional or local climate changes despite uncertainty in the dynamical cause."

We note that it is difficult to tie precipitation changes across our domain and South America to one specific dynamical forcing such as changes in the SWW. To do so would require a separate analysis and dedication to another paper. However, we have added some additional analysis, which we will add to <u>a supplement</u>, regarding how TraCE-21ka simulates changes in large atmospheric scale circulation and associated changes in the SWW. We analyzed outputs of 925 hPa zonal winds and computed moisture flux convergence to help fill gaps in our current manuscript. Below is text that will be added to our Discussion section 4.1.

** Please note: We have attached figures at the end of this document which we cite here in our response. These figures will be added to a supplement.

"We analyzed outputs of the JJA 925 hPa zonal wind as the mean over 500 yr periods from TraCE-21ka for the LGM (22-21ka), 18ka (18.5-18ka), 16ka (16.5-16ka), 14ka (14.5-14ka), and 12ka (12.5-12ka) and the Preindustrial (PI ; Figures S3 A-E). Across our model domain and to its south, relative to the PI, zonal winds are stronger during the LGM (Figure S3A first and second column), with a southerly displacement compared to the PI. During 18ka (Figure S3B), the zonal wind increases in strength relative to the PI, with the stronger winds having wider latitudinal coverage, particularly across our model domain. While the mean position of the SWW is poleward at 18ka relative to the PI (Jiang and Yan, 2022), across Patagonia the simulated position of the maximum zonal wind is at the same latitudinal band as the PI. At 16ka, the zonal wind is stronger across our domain and Patagonia (Figure S3C) relative to the PI, although not as large as the differences during 18ka. By 14ka, the strength in the zonal winds across Patagonia and our model domain are similar to slightly stronger than the PI (Figure S3D), however, the zonal wind maximum is situated more equatorward across our model domain relative to the PI. By 12ka (Figure S3E), the zonal wind is similar to slightly weaker than the PI across our model domain, although it is stronger relative to the PI to the south of our model domain across central and southern Patagonia. The position of the maximum zonal winds is also displaced further south relative to the PI. These changes in strength and position of the simulated SWW during the last deglaciation are similar to the findings of Jian and Yan (2020). They evaluated the change in the SWW during the last 21,000 years using TrACE-21ka and find that relative to the Preindustrial (PI), TraCE-21ka simulates a more poleward subtropical and subpolar jet over the Southern hemisphere at the LGM. During the remainder of the LGM and last deglaciation, the overall position of the SWW migrates northward in TraCE-21ka, with poleward displacements during Heinrich Stadial 1 (HS1), equatorward displacements during the Antarctic Cold Reversal (ACR), and poleward displacements during the Younger Dryas (YD), similar to what our analysis finds.

Additionally, we evaluated the JJA low-level (850 hPa) moisture flux convergence from TraCE-21ka (MFC; see supplemental), which is influenced by the mean flow and transient eddies in the extratropical hydrologic cycle (*Peixoto and Oort,* 1992). During the LGM, MFC increases across our model domain relative to the PI, and increases during 18ka consistent with a convergence of the mean flow moisture fields relative to the PI (Figure S4 A,B). During the LGM and 18ka, we note that TraCE-21ka simulates higher JJA precipitation anomalies (relative to the PI) across our model domain (Figure 9). While our analysis cannot directly constrain the source of the positive precipitation anomalies (e.g., mean flow, storms), the SWW simulated in TraCE-21ka strengthens across our model domain (Figure S3 A,B) coincident with the increases in MFC, which may contribute to the positive precipitation anomalies at these time intervals (Figure 9). By 16ka, there is increased divergence in the 925 hPa winds and moisture relative to the PI (Figure S4 C). Decreased MFC relative to the PI coincides with a reduction in precipitation across our model domain that are similar or less than the PI (Figure 9). We note that the ice thickness boundary conditions used in the TraCE-21ka come from the Ice5G reconstruction (Peltier, 2004), which has the PIS being deglaciated completely at 16ka. However, our analysis cannot decompose whether the simulated changes in precipitation and MFC are a consequence of the coupling between regional atmospheric circulation and the ice thickness boundary conditions used in TraCE-21ka or if these changes represent wider interactions with changes in hemispheric atmospheric circulation. By 14ka, and during the ACR, MFC increases relative to the PI (Figure S4D). This is consistent with a simulated equatorward migration of the SWW as shown in Jiang and Yan (2020) and our analysis (Figure S3D), and positive anomalies in precipitation across our model domain relative to the PI (Figure 9). By 12ka, precipitation across our model domain is reduced relative to the PI (Figure 9), and TraCE-21ka simulates a reduction in the MFC as well as a poleward migration of the SWW (Figure S3E; Jiang and Yan, 2020).

When examining the changes in proxy records of precipitation across the CLD, there is reasonable agreement with the changes in precipitation simulated by TraCE-21ka. Moreno et al. (1999;2004; 2015) and Moreno and Videla (2016) find that wetter than present day conditions existed across the CLD during the LGM and early deglaciation which is consistent with the precipitation anomalies simulated in TraCE-21ka (Figure 9). These changes in paleoclimate proxies are attributed to an intensified storm track associated with an equatorward shift of the SWW (Moreno et al. 1999; 2004; 2015). While TraCE-21ka instead simulates a poleward shift of the SWW during these time intervals, increases in precipitation and the intensification of the storm track as inferred by Moreno et al. (2004; 2015) may also be consistent with a strengthening of the SWW as simulated by TraCE-21ka during these intervals (Figure S3 A,B; Rojas et al., 2009; Sime et al., 2013; Kohfeld et al., 2013). Moreno et al. (2015) note that rapid warming ensues across the CLD around 17,800 cal yr BP, which is similar to the timing of deglacial warming as simulated by TraCE-21ka around 18.5 ka (Figure 8). Coincident with this rapid temperature rise, Moreno et al. (2015) note a shift from hyper humid to humid conditions which aligns well with decreases in the simulated precipitation in TraCE-21ka across our model domain (Figure 9). Lastly, Moreno et al. (2004; 2015) find that colder and wetter conditions occur across the CLD during the ACR, and infer an equatorward expansion of the SWW as a potential cause. While TraCE-21ka simulates an abrupt and short ACR, it does simulate an equatorward expansion of the SWW (Figure S4 D; Jian and Yan, 2020), associated cooling (Figure 8), and increases in precipitation (Figure 9) that agree with the proxy data."

Ref:

Jiang, N., Yan, Q. Evolution of the meridional shift of the subtropical and subpolar westerly jet over the Southern Hemisphere during the past 21,000 years. 2020. Quaternary Science Reviews. 246. https://doi.org/10.1016/j.quascierev.2020.1066544.

Peixoto, J. P., and A. H. Oort (1992), Physics of Climate, American Institute of Physics, 520 pp.

W.R. Peltier, 2004. Global Glacial Isostasy and the Surface of the Ice-Age Earth: The ICE-5G (VM2) Model and GRACE, Ann. Rev. Earth and Planet. Sci., 32, 111-149.

- **2b) It remains unexplained what drives the increased winter precipitation in TRACE-21ka between 22 and 18 ka relative to the preindustrial (PI). Are the inferred driving mechanisms supported by at least one of the PMIP4 models? It is also unclear why the inferred deviation between winter precipitation anomalies in the north and south disappears after 16 ka. Finally, what mechanisms drive dips is the winter precipitation relative to the PI after 16 ka?**

We would like to refer the reviewer to our discussion in 2a. We have done more analysis of the TraCE-21ka outputs and with existing literature. The discussion provides more detail on the possible controls on the simulated changes in precipitation during these time intervals. Likewise, we have added additional context as to how the changes simulated in TraCE-21ka relate to the paleoclimate records across the CLD.

- **2c) While the idea of using TRACE-21ka for the applications in Patagonia is new, this climate forcing suffers from a very low spatial resolution (T31) that is suboptimal for a region with such steep topography and its regional performance has not been validated against any paleoclimate proxy data in South America or neighboring areas. The lack of validation and interpretation of the inferred climate time series from TRACE-21ka against existing sediment and ice core records and other proxies, both regional and semi-hemispheric, is a flaw of the study. It is incorrect that such reconstructions are missing in the region, and at least some effort could be made to compare with the signals reconstructed from the West Antarctic ice core data.**

Large, multi-proxy reconstructions from papers by He and Clark 2022, Liu et al. 2009, He et al. 2011, Shakun et al. 2015, Shakun et al. 2012, Marcott et al. 2013, etc. have all demonstrated good agreement between TRACE 21k and paleo proxy data. These studies include a wide variety of paleo-proxy data that include West Antarctic and proxy records from South America. Our own analyses (unpublished – see figure below of temperature reconstruction) has also show generally good agreement between TRACE 21k and existing records from the last glacial to present in the Southern Hemisphere. Additionally, we have now undertaken analyses in this paper (see Discussion above 2A) which further demonstrates the agreement between the modeling results and local paleo-precipitation and temperature proxies.

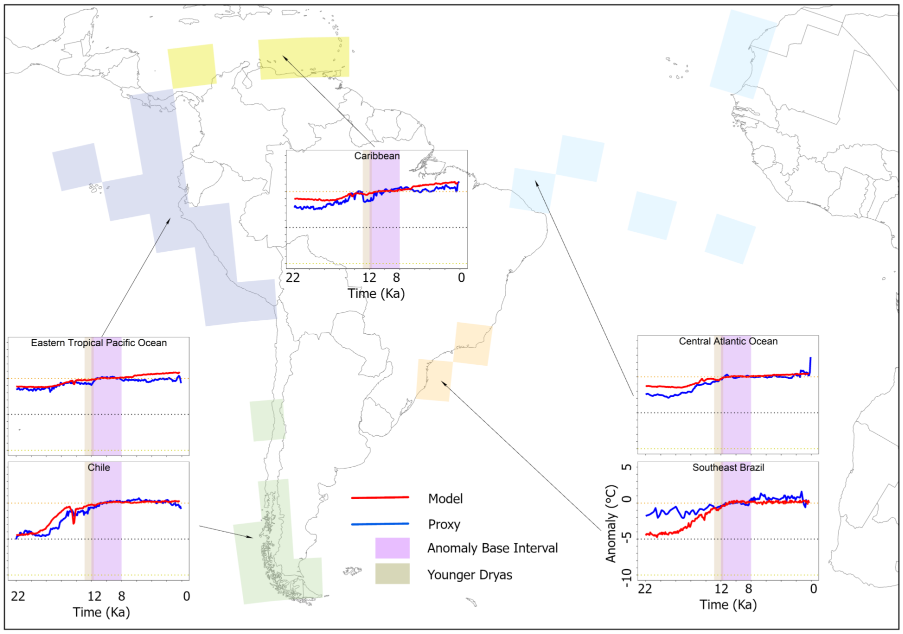

- **3. Methodology flaws and missing information: There are quite some simplifications and limitations in the methodology and experimental design that must be considered in a greater detail.**
- **3a) The impacts of the missing treatment of ice temperature and viscosity on the ice sheet dynamics must be demonstrated as negligible. Currently it is dismissed as a factor through weak arguments. The computational efficiency may be a good reason for model simplifications but not at the cost of the non-physical model outcomes. I see the need for sensitivity experiments that would quantify the impacts and related uncertainties in the study's conclusions. Also, a reference supporting the statement in lines 135-136 is painfully missing, including the considerations that in areas with such thin lithosphere and high geothermal flux, temperate basal conditions do not always translate into vertically temperate glacier regimes.**

In order to test the validity of our assumption of a largely temperate based ice sheet across this domain, we calculate ice temperature at the LGM, assuming the ice sheet is in a steady-state thermal equilibrium following Serrousi et al. (2013). This methodology has been used for numerous applications in Greenland and Antarctica to calculate the thermal conditions of the ice sheets (Seroussi et al., 2013; MacGregor et al., 2016; Goelzer et al., 2020; Seroussi et al., 2020). We use our modeled LGM ice sheet state for the SynTraCE-21ka simulation (ice sheet geometry) to calculate the thermal conditions of the ice sheet. This formulation, outlined in Seroussi et al. (2013) uses an enthalpy formulation from Aschwanden et al. (2012) that includes both temperate and cold ice. LGM air temperature is imposed at the surface and geothermal heat flux is applied at the base (100 mW m−2 mean from Hamza and Vieira, 2018). For this step, we extrude our 2D model to 3D, with the model for the thermal state calculation having 20 layers.

Here we show the simulated Steady State Basal Temperatures (A) and the simulated Depth Averaged Steady State temperatures (B). See below for figures.

The ice sheet is mainly warm based (figure A; below) with temperatures near 0 degrees Celsius, with exception for some of the high peaks where ice cover is thin enough for the colder surface temperatures to diffuse and advect downward. The depth averaged temperature (figure B; below) shows that the majority of the ice sheet is between -1 to 0 degrees Celsius, with the mean of the depth averaged temperature being -0.41 degrees Celsius. There are some exceptions, where colder ice seems to be advected downstream from the colder based high peaks (in figure A), however, we must note that these simulated temperatures are likely an underestimate as they do not account fully for frictional heating that would occur if the 3D thermal model was run transiently (mass transport and stress balance) to steady state.

Therefore, based on this additional analysis, we think that our assumption in setting the ice temperature in our 2D model to -0.2 degrees Celsius is justified. We will add this analysis and text to the supplement and reference it in our text discussion on the thermal state of the ice sheet (section 2.1 Ice Sheet Model).

We have added a reference in lines 140-141 and adjusted the text to reflect this:

"Although geomorphological evidence suggests that while southernmost glaciers across the PIS may have been temperate with warm based conditions during the LGM, there may have been periods where ice lobes were polythermal (Darvill et al., 2016). However, recent ice flow modelling (Leger et al., 2021) suggests that varying ice viscosity mainly impacts the accumulation zone thickness in simulations of paleoglaciers in Northeastern Patagonia, with minimal impacts on overall glacier length and extent. Accordingly, based on sensitivity tests (see supplement), our model is 2-dimensional and we do not solve for ice temperature and viscosity allowing for increased computational efficiency."

We additionally note that geomorphological and topographic evidence is suggestive of widespread temperate ice conditions across the north Patagonian batholith. This is depicted in abraded surfaces at different elevations ranging from 900-2000 m.a.s.l, including the highest peaks. Glacially polished bedrock surfaces were recognized through ground-validating fieldwork (Romero et al., 2023 INQUA Abstract), suggesting that the ice sheet could have been at the pressure-melting point at its base, ruling out signs of cold based conditions. Moreover, results from thermochronology studies revealed that higher latitudes in Patagonia experienced reduced late Cenozoic erosion in comparison to northern sites (Thomson et al., 2010). This study noted that northern sites of the Patagonian Andes did not exhibit signs of glacial protection from erosion, indicating that southern sites must have experienced spatially restricted glacier basal flow. This kind of glacial protection of the landscape has been determined to occur in polar regions mostly. Therefore, we suggest that geomorphic evidence and thermochronological studies highlight that northern Patagonia would have exhibited temperate ice conditions.

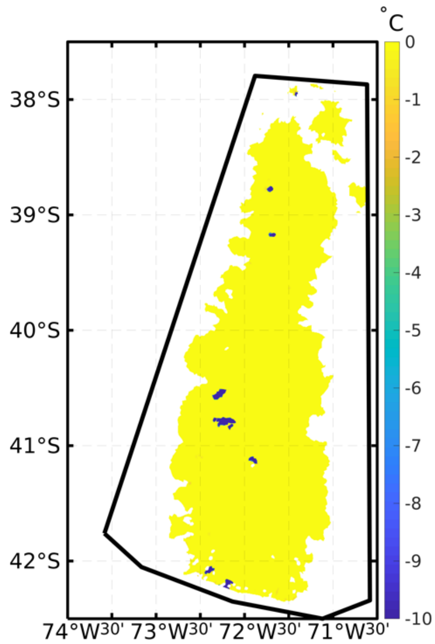

Figure A. Simulated Steady State basal temperature in degrees Celcius.

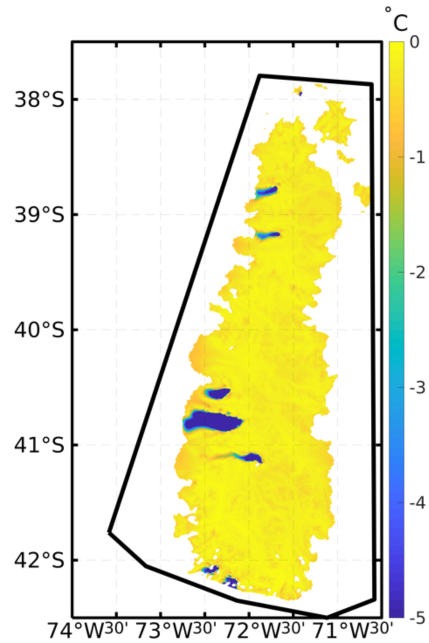

Figure B. Simulated depth averaged ice temperature in degrees Celcius.

References:

Aschwanden, A., Bueler, E., Khroulev, C., and Blatter, H.: An enthalpy formulation for glaciers and ice sheets, J. Glaciol., 58, 441–457, https://doi.org/10.3189/2012JoG11J088, 2012.

Darvill, C.M., Stokes, C.R., Bentley, M.J., Evans, D.J.A., Lovell, H. Dynamics of former ice lobes of the southernmost Patagonian Ice Sheet based on a glacial landsystems approach. Journal of Quaternary Science. 32,6,857-876. https://doi.org/10.1002/jqs.2890

Goelzer, H., Nowicki, S., Payne, A., Larour, E., Seroussi, H., Lipscomb, W. H., Gregory, J., Abe-Ouchi, A., Shepherd, A., Simon, E., Agosta, C., Alexander, P., Aschwanden, A., Barthel, A., Calov, R., Chambers, C., Choi, Y., Cuzzone, J., Dumas, C., Edwards, T., Felikson, D., Fettweis, X., Golledge, N. R., Greve, R., Humbert, A., Huybrechts, P., Le clec'h, S., Lee, V., Leguy, G., Little, C., Lowry, D. P., Morlighem, M., Nias, I., Quiquet, A., Rückamp, M., Schlegel, N.-J., Slater, D. A., Smith, R. S., Straneo, F., Tarasov, L., van de Wal, R., and van den Broeke, M.: The future sea-level contribution of the Greenland ice sheet: a multi-model ensemble study of ISMIP6, The Cryosphere, 14, 3071–3096, https://doi.org/10.5194/tc-14-3071-2020, 2020.

Seroussi, H., Nowicki, S., Payne, A. J., Goelzer, H., Lipscomb, W. H., Abe-Ouchi, A., Agosta, C., Albrecht, T., Asay-Davis, X., Barthel, A., Calov, R., Cullather, R., Dumas, C., Galton-Fenzi, B. K., Gladstone, R., Golledge, N. R., Gregory, J. M., Greve, R., Hattermann, T., Hoffman, M. J., Humbert, A., Huybrechts, P., Jourdain, N. C., Kleiner, T., Larour, E., Leguy, G. R., Lowry, D. P., Little, C. M., Morlighem, M., Pattyn, F., Pelle, T., Price, S. F., Quiquet, A., Reese, R., Schlegel, N.-J., Shepherd, A., Simon, E., Smith, R. S., Straneo, F., Sun, S., Trusel, L. D., Van Breedam, J., van de Wal, R. S. W., Winkelmann, R., Zhao, C., Zhang, T., and Zwinger, T.: ISMIP6 Antarctica: a multi-model ensemble of the

Antarctic ice sheet evolution over the 21st century, The Cryosphere, 14, 3033–3070, https://doi.org/10.5194/tc-14-3033-2020, 2020.

MacGregor, J. A., Fahnestock, M. A., Catania, G. A., Aschwanden, A., Clow, G. D., Colgan, W. T., Gogineni, S. P., Morlighem, M., Nowicki, S. M., Paden, J. D., and Price, S. F.: A synthesis of the basal thermal state of the Greenland Ice Sheet, J. Geophys. Res.-Earth, 121, 1328–1350, 2016.

Romero, M., Cuzzone, J.K., Jones, A.G., Bushmaker, S., Marcott, S.A. Post-Glacial dynamics of the Patagonian Ice Sheet across the Southern Volcanic Zone. In: XXI INQUA Congress, July 14th – 20th 2023, Sapienza University of Rome, Italy

Seroussi, H., Morlighem, M., Rignot, E., Khazendar, A., Larour, E., & Mouginot, J. (2013). Dependence of century-scale projections of the Greenland ice sheet on its thermal regime. Journal of Glaciology, 59(218), 1024–1034. https://doi.org/10.3189/2013JoG13J054

Hamza, V. M. and Vieira, F.: Global heat flow: new estimates using digital maps and GIS techniques, International Journal of Terrestrial Heat 490 Flow and Applied Geothermics, 1, 6–13, https://doi.org/10.31214/ijthfa.v1i1.6, 2018

Thomson, Stuart N., et al. "Glaciation as a destructive and constructive control on mountain building." *Nature* 467.7313 (2010): 313-317.

- **3b) It must be at least discussed how the absence of the Glacial Isostatic Adjustment (GIA) modeling is impacting the model reconstructions and conclusions of this study. While I do not fully agree with the referee 1 that the GIA is a controlling factor, given the high uncertainties in the model parameters, parameters of the downscaling procedure and external forcings, I agree with their arguments that this limitation of the model must be addressed in a much more thorough manner. Here I refer the authors to the detailed suggestions of the referee 1.**

We would kindly point Reviewer 2 to our response to Reviewer 1 where we address these concerns and revisions in full.

- **3c) Given the steep topographic gradients that dominate regional climate, it is not discussed enough how the choice of such a small model domain compared to the grid sizes of the climate models is impacting the outcomes of the modeling experiments, hugely inflating the role of the chosen parameters for downscaling.**

Our model domain encompasses 4 TrACE-21ka gridcells. While the climate model outputs cannot adequately capture the steep topographic gradients as expressed by the reviewer, we apply anomalies of climatologies from the climate models and not the raw data. The anomalies are applied onto a high-resolution reanalysis product (CR2MET), and the temperature and precipitation are adjusted following lapse rate adjustments (temperature) and elevation desertification (for precipitation). Please see comment 3E below. We apply a standard modeling approach (Pollard et al., 2012; Seguinot et al., 2016; Golledge et al., 2017; Tigchlaar et al., 2019; Clark et al., 2020; Briner et al., 2020; Cuzzone et al., 2022; Yan et al., 2022): using climate model output allows us to capture more spatial variability that accounts for changes in climate due to large scale atmospheric circulation change versus, for instance, ice core scaling techniques which only rely on scaling a present day climatology based on variations from a far field site. While perfectly acceptable, ice core scaling techniques often take remote ice cores (often from Greenland or Antarctica) changes in temperature and apply these anomalies to a large geographical area; for example, see Seguinot et al., 2016 (citation below in 3E). While it may be more beneficial to have higher resolution climate model output that accounts for higher resolution topography, our approach is sound and still allows for an improved understanding of the possible deglaciation of the PIS across this region especially given the large uncertainty in the geologic reconstruction during the later deglaciation. Additionally, thanks to the Reviews suggestion to compare TraCE-21ka to regional proxies in the CLD, we are more confident that changes simulated in TraCE-21ka match well with the proxy records.

Likewise, we do not feel we have inflated the role of chosen parameters. For the transient (last deglaciation) simulations, we need to initialize our model. This requires some parameter choice such that the simulated LGM ice sheet fits some "observed" state. In this case (as described in comment 3D below), our simulated LGM ice sheet using the TraCE-21ka climate has a good fit to the PATICE LGM ice area (within 5%; figure 11), and therefore we can say that the model achieves a good fit to the "observed" LGM extent from PATICE. We then keep those parameters constant and apply the deglacial climate changes to simulate the last deglaciation across our model domain. This approach is similar to how the community simulates future or past ice sheet change for glaciers or Greenland/Antarctica. Parameter choices need to be made that satisfy an initial simulated ice state against some observable, giving confidence that the simulated transient changes are robust.

- **3d) Referring to Yan et al.'s paper for the choice of internal model parameters is a poor practice since this paper utilizes model parameters that are fine-tuned to support their desired outcomes rather than parameters supported by observational evidence from glaciated regions on our planet today. This brings us to a question – how have the choices of lapse rate and PDD model parameters impacted the modeled extents and volumes of the ice sheet?**

We kindly point the reviewer to a citation we also listed (Fernandez et al., 2016) in text. They list published model parameter choices for the positive degree day approach as it applies to modeling contemporary and historical glacier change across South America. Parameter values vary between studies, however, the values we have chosen for this study are within the range of values used across this region, and are therefore supported by observational and modeled evidence from glaciated regions in South America.

Because our transient ice modelling across the last deglaciation uses the TrACE-21ka climate outputs, our degree day and lapse rate parameters were chosen so that the simulated LGM ice area was in close agreement with the reconstructed PATICE area at the LGM (within 5% of reconstructed ice area for PATICE; Figure 11). This provides confidence in our modeled LGM state using the TrACE-21ka climate outputs. And for the transient deglacial simulations, these parameters remain constant and only the climate forcing varies through the last deglaciation simulation. Again, we follow standard practice in ice sheet modelling: that is, once a model is initialized, and parameters are chosen that provide a good match between a modeled and observed LGM state, those parameters are held constant during transient simulations.

We can add text in Section 2.3 Surface Mass Balance (line 223), to reflect these choices in model parameters: "Using these parameter values, we arrive at a simulated LGM ice sheet area matches well (within 5%) to the reconstructed ice area from PATICE (see Figure 11) for the simulation using the TraCE-21ka climate forcing."

- **3e) The resulting ice sheet geometries presented in Figure 5 in response to different PMIP4 climate forcings and in combination with the listed Positive Degree Day (PDD) parameters are surprising, to say the least. Both AWI and MPI climate model outputs must be modified significantly to enable the growth of an ice sheet in this area. I am missing the information about the model parameters adapted in this study – for example, what is the daily temperature standard deviation in the PDD model? This is a principal parameter that shapes glacier and snow melt. A more detailed description of the downscaling procedure is also needed. For example, how was precipitation downscaled/corrected? How was the ice sheet boundary forcing in the climate models accounted for when downscaling? A table in the appendix with all major model parameters and a detailed method description would be much appreciated.**

We have added this to section 2.3: "The hourly temperatures are assumed to have a normal distribution, of standard deviation 3.5 degrees Celsius around the monthly mean." Our other mass balance parameters are listed in that section but if a table is easier to digest, than we will be more than happy to include one.

We discuss the application of the climate forcings in Section 2.4. We use a common approach in numerical ice flow modeling to simulate ice behavior across paleoclimate timescales. We point the reviewer to Section 2.4.

We have added additional citations in Section 2.4 to support this: "In order to scale monthly temperature and precipitation across the LGM and last deglaciation we applied a commonly used modeling approach (Pollard et al., 2012; Seguinot et al., 2016; Golledge et al., 2017; Tigchlaar et al., 2019; Clark et al., 2020; Briner et al., 2020; Cuzzone et al., 2022; Yan et al., 2022)" As described in the text, the lapse rate is used to down scale the temperatures onto the resulting topography (ice surface).

To scale precipitation an elevation-dependent desertification is included (Budd and Smith, 1981) which reduces precipitation by a factor of 2 for every kilometer change in ice sheet surface elevation. We have added this text to section 2.4: "An elevation-dependent desertification is included (Budd and Smith, 1981) which reduction in precipitation by a factor of 2 for every kilometer change in ice sheet surface elevation (Budd and Smith, 1981) ."

References

Golledge, N. R., Thomas, Z. A., Levy, R. H., Gasson, E. G. W., Naish, T. R., McKay, R. M., Kowalewski, D. E., and Fogwill, C. J.: Antarctic climate and ice-sheet configuration during the early Pliocene interglacial at 4.23 Ma, Clim. Past, 13, 959–975, https://doi.org/10.5194/cp-13-959-2017, 2017.

Tigchelaar, M., Timmermann, A., Friedrich, T., Heinemann, M., and Pollard, D.: Nonlinear response of the Antarctic Ice Sheet to late Quaternary sea level and climate forcing, The Cryosphere, 13, 2615–2631, https://doi.org/10.5194/tc-13-2615-2019, 2019.

Clark, P.U., He, F., Golledge, N.R., Mitrovica, J.X., Dutton, A., Hoffman, J.S., and Dendy, S., 2020, Oceanic forcing of penultimate deglacial and last interglacial sea-level rise: Nature, v. 577, p. 660–664, doi:10.1038/s41586-020-1931-7.

Budd, W. F. and Smith, I.: The growth and retreat of ice sheets in response to orbital radiation changes, Sea Level, Ice, and Climatic Change, 131, 369–409, 1981.

Seguinot, J., Rogozhina, I., Stroeven, A. P., Margold, M., and Kleman, J.: Numerical simulations of the Cordilleran ice sheet through the last glacial cycle, The Cryosphere, 10, 639–664, https://doi.org/10.5194/tc-10-639-2016, 2016.

- **3f) In Section 2.5 (lines 225-229), the lake calving process is presented as a brand-new feature of glacier models that has its own unique challenges compared to the ocean-driven calving. Could the authors shortly explain the differences and why it is so hard to implement this process in their model?**

It is not directly difficult to include lake calving in the model simulations per say. We currently do not have a scheme to form proglacial lakes in ISSM, which is likely what happened during the deglaciation across the CLD – as proglacial lakes formed during ice retreat. We could instead impose lakes that are always present throughout the simulation. However, there are uncertainties surrounding the resolution needed to capture such grounding line migrations as the ice front advances and retreats across the lakes. In our work applying ISSM to Greenland, we find that model resolutions need to be <1km in order to accurately capture the grounding line migration (Seroussi and Morlighem, 2018). Additionally, there is uncertainty regarding what calving criteria is best suited for calving in proglacial lakes. In ISSM we typically use the Von Misses calving criteria in areas such as Greenland. We are not sure what values for the stress thresholds should be adequate for proglacial lake calving since we have not done any tests to benchmark them like we have done for the Greenland Ice sheet. Many models (Hinck et al., 2022; Quiquet et al., 2021) that incorporate proglacial lake calving use a simple thickness criterion from which calve off ice. While suitable, we would need to do additional uncertainty tests to determine how much values in this criterion influence the ice retreat. We would also like to note that proglacial lake calving across the CLD is the focus of current and future work with ISSM. For this work we will be using a local scale, very high-resolution ice model and will try and address some of the questions raised above.

Ref:

Seroussi, H. and Morlighem, M.: Representation of basal melting at the grounding line in ice flow models, The Cryosphere, 12, 3085–3096, https://doi.org/10.5194/tc-12-3085-2018, 2018.

We acknowledge that not including calving on proglacial lakes represents limitation in our deglacial simulations and we have added text to a new Limitations section (4.3) in the Discussion.

We have added some text in the Limitations section (Section 4.3).

"Across most of our domain, there is evidence for an advance of piedmont glaciers across glacial outwash during the LGM, which formed the physical boundary for some of the existing terminal moraines around the lakes within the CLD (Bentley, 1996; Bentley, 1997). The formation of ice-contact proglacial lakes likely occurred as a function of deglacial warming and ice retreat Bentley (1996). Where there were proglacial lakes along the westward ice front in the CLD, evidence suggests that ice was grounded during the LGM (Lago Puyehue; Heirman et al., 2011). During deglaciation, iceberg calving into the proglacial lakes may have occurred (Bentley 1996,1997; Davies et al., 2020), with evidence suggesting that local topography and calving may have controlled the spatially irregular timing of abandonment from the terminal moraines surrounding the proglacial lakes (Bentley, 1997). Recent glacier modelling (Sutherland et al., 2020) suggests that inclusion of ice-lake interactions may have large impacts on the magnitude and rate of simulated ice front retreat, as ice-lake interactions promote greater ice velocities, ice flux to the grounding line, and surface lowering. However, across our region Heirman et al. (2011) indicate that is not well constrained how the proglacial lakes in the CLD may have influenced local deglaciation, and more geomorphic data is needed. Therefore, because the inclusion of ice-lake interactions is relatively novel for numerical ice flow modeling (Sutherland et al., 2020; Quiquet et al., 2021; Hinck et al., 2022), we choose to not model the evolution and influence of proglacial lakes on the deglaciation across this model domain. Given this limitation, our simulated magnitude and rate of ice retreat at the onset of deglaciation may be underestimated, especially when looking at local deglaciation along these proglacial lakes. Although we do not think that these processes would greatly influence our conclusions regarding the role of climate on the evolution of the PIS is the CLD region and the simulated ice retreat history, future work is required to assess the influence of proglacial lakes in this region. "

- **3g) The design of the sensitivity analysis is incomplete, further emphasizing the disconnect between the LGM and transient experiments. This is an area where stronger connections between the two sets of experiments can be built by for example, also testing precipitation anomalies from at least some of the utilized PMIP4 models. It would be also beneficial to test how the deglaciation would look like if the PI precipitation and present-day observed precipitation rates were used to drive the deglaciation run. It would allow this study to decouple the impacts of higher-than-PI winter precipitation prior to 18 ka and lower-than-PI winter precipitation after 16 ka the pace of the deglaciation.**

We agree with the reviewer that additional sensitivity tests are needed to better support the role of precipitation in modulating deglacial ice retreat across the CLD. Since we decided to remove the PMIP4 simulations from this manuscript, we added 2 additional simulations using the TraCE-21ka model output. In the current manuscript we have 2 transient simulations. One where the TraCE-21ka climate boundary conditions vary through time (listed as #1 below and referred to as the **main simulation**) and a second simulation where we fix the precipitation during the transient simulation to be equivalent to the monthly mean from 22ka to 20ka (#4 below). Taking the reviewers suggestion, we conduct 2 more transient simulations (#2 and #3 below). In all of these sensitivity experiments (#2-4 below and referred to as sensitivity experiments 2-4), temperature varies across the last deglaciation but precipitation remains fixed at the given magnitude for a particular chosen time interval.

List of simulations:

1) Climate boundary conditions (temperature and precipitation) vary through time (denoted as the **main simulation**).
2) Monthly precipitation is held constant at the preindustrial mean. This is what the reviewer suggests above.
3) Monthly precipitation is held constant at the mean 12.5 ka-12 ka values. From figure 9 in the current manuscript, we see that this is a period of reduced precipitation relative to the preindustrial (~7% reduction).
4) Transient simulation where the monthly precipitation is held constant to the 22-20 ka mean from TraCE-21ka, which is roughly 10% higher than preindustrial values across the Northern portion of the model domain (North of 40°S).

As the reviewer suggests, sensitivity experiments 2 and 4 allows us to better assess the impacts of higher than PI winter precipitation prior to 18ka, while experiment 3 allows us to assess how a reduced precipitation during the deglaciation influences the overall pacing of ice retreat.

The results are shown below as the difference in the simulated deglaciation between the sensitivity experiments (#2,3,4) and the main simulation (#1). The blue colors indicate that the simulated deglaciation for the sensitivity experiments are slower than the main simulation, and the red colors indicate that the simulated deglaciation for the sensitivity experiments are faster than the main simulation.

In Figure SA below, the difference in the deglaciation age between sensitivity experiment 2 and the main simulation is shown, where precipitation is held constant at the preindustrial value. Please note we call this Figure S, but will give it an appropriate Figure # in the revised manuscript. Across our model domain, wintertime precipitation during the preindustrial is reduced compared to the early deglaciation (22 ka to 18ka) and is similar to slightly higher particularly south of 40°S after 18 ka (Figure 9 from current manuscript). When holding precipitation constant at the preindustrial value through the last deglaciation, we notice that ice retreats faster across most portions of the model domain, particularly along the ice margins and in the northern sector. In the southern portion of our model domain, where the relative changes in deglacial precipitation relative to the preindustrial are smaller, the difference in simulated deglaciation age are also smaller. In general, the pace of deglaciation increases by up to 1 kyr compared to the main simulation, with many locations experiencing deglaciation 200-600 yrs earlier than the standard simulation.

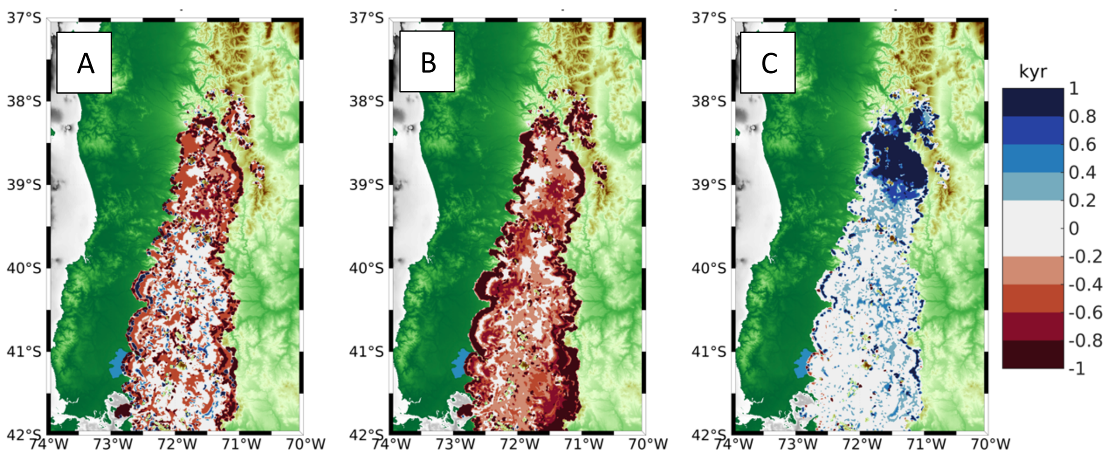

Figure S. A) The difference in the simulated deglaciation age between sensitivity experiment 2 and the main simulation. B.) The difference in the simulated deglaciation age between sensitivity experiment 3 and the main simulation. C.) The difference in the simulated deglaciation age between sensitivity experiment 4 and the main simulation. Blue colors indicate slower ice retreat for the sensitivity experiments compared to the main simulation, while red colors indicate faster ice retreat for the sensitivity experiments compared to the main run.

In Figure SB the difference in the deglaciation age between sensitivity experiment 3 the main simulation and is shown, where precipitation is held constant at the monthly mean 12.5 ka- 12 ka value. Winter precipitation during 12.5 ka – 12 ka is reduced modestly by up to 7% relative to the preindustrial across the model domain (see Figure 9 current manuscript). Ice retreats faster across most portions of the model domain, particularly along the ice margins through the interior. Deglaciation along the margins occurs >1 kyr in many locations, and between 200 yrs to 1 kyr faster across portions of the ice interior.

In Figure SC the difference in the deglaciation age between sensitivity experiment 4 and the main simulation is shown, where precipitation is held constant at the monthly mean 22 ka- 20 ka value. This simulation is discussed in our current manuscript (current Figure 7B), but here we show the difference from the main simulation. Winter precipitation during 22 ka – 20 ka is increased by up to 10% relative to the preindustrial (Figure 9 current manuscript) across the northern portion of the model domain (North of 40S), but is similar to preindustrial values across the southern portion of our model domain (South of 40S). As discussed in the current manuscript, with higher precipitation across the northern portion of the model domain, ice retreats slower during the last deglaciation relative to our main simulation by >1 kyr (and in some locations up to 2 kyr).

Much of the deglacial winter precipitation anomalies are within 10% of the preindustrial values (Figure 9). While temperature is the main driver of ice retreat (as shown by previous studies cited in the manuscript), these sensitivity studies suggest that modest changes in precipitation can alter the pace of ice retreat. While we have shown with the analysis of the TraCE-21ka outputs that the circulation changes and precipitation anomalies simulated across the last deglaciation qualitatively match well with paleoclimate proxies across the CLD (please see our discussion to RC 2A above and associated figures provided), many of those paleoclimate proxies indicate that the LGM and early deglaciation may have been up to 2 times wetter than present day (Moreno et al., 1999; 2015). Therefore, because the anomalies of precipitations during the early deglaciation relative to the preindustrial as simulated by TraCE-21ka are smaller than those anomalies in precipitation found in the proxy records, we can deduct from our sensitivity analysis here that precipitation across the CLD, forced by proposed changes in the SWW (Moreno et al., 1999;2015) may have helped offset melt from deglacial warming thereby influencing the pacing of early deglacial ice retreat in this region.

*How we plan to revise this section. Please note we refer to the new figure above as Figure S. We will give this the appropriate figure # in the updated manuscript:

We will plan to Revise Figure 7 and instead just show the resulting deglaciation age for the main simulation. Then in section 3.2.2 (Sensitivity Tests), we will add the panel figure above, which shows the results from the sensitivity experiments where precipitation is held fixed across the last deglaciation experiments. Text below will be added to section 3.2.2 as:

"To better assess how changes in precipitation may modulate the deglaciation across the CLD we perform additional sensitivity tests. We refer to the simulation discussed above as our *main run*, where the climate boundary conditions of temperature and precipitation varied temporally and spatially across the last deglaciation. Three more simulations are performed where temperature is allowed to vary across the last deglaciation, but precipitation remains fixed at a given magnitude for a particular time interval. Each experiment is listed below as:

1) Monthly precipitation is held constant at the preindustrial mean. Displayed in Figure 9, wintertime preindustrial precipitation reduced compared to the period 22 ka to 18 ka, but is higher than what is simulated after 18 ka for the exception of the ACR at 14.5 ka.
2) Monthly precipitation is held constant at the mean 12.5 ka-12 ka values. Displayed in Figure 9 this is a period of reduced precipitation relative to the preindustrial (~7% reduction).
3) Monthly precipitation is held constant to the 22-20 ka mean, which is roughly 10% higher than preindustrial values across the Northern portion of the model domain (North of 40°S).

In Figure SA, the difference in the deglaciation age between sensitivity experiment 1 and the main simulation is shown, where precipitation is held constant at the preindustrial value. Across our model domain, wintertime precipitation during the preindustrial is reduced compared to the early deglaciation (22 ka to 18ka) and is similar to slightly higher particularly south of 40°S after 18 ka (Figure 9). When holding precipitation constant at the preindustrial value through the last deglaciation, we notice that ice retreats faster across most portions of the model domain, particularly along the ice margins and in area north of 40°S. In the southern portion of our model domain (south of 40°S), where the changes in deglacial precipitation relative to the preindustrial are lower (Figure 9), the difference in simulated deglaciation age are also smaller. In general, the pace of deglaciation increases by up to 1 kyr compared to the main simulation, with many locations experiencing deglaciation 200-600 yrs earlier than the main simulation.

In Figure SB the difference in the deglaciation age between sensitivity experiment 2 and the main simulation is shown, where precipitation is held constant at the monthly mean 12.5 ka- 12 ka value.

Winter precipitation during 12.5 ka – 12 ka is reduced modestly by up to 7% relative to the preindustrial across the model domain (Figure 9). Ice retreats faster across most portions of the model domain, along the ice margins through the interior. Deglaciation along the margins occurs >1 kyr in many locations, and between 200 yrs to 1 kyr faster across portions of the ice interior.

In Figure SC the difference in the deglaciation age between sensitivity experiment 3 and the main simulation is shown, where precipitation is held constant at the monthly mean 22 ka- 20 ka value. Winter precipitation during 22 ka – 20 ka is increased by up to 10% relative to the preindustrial (Figure 9) across the northern portion of the model domain (north of 40°S), but is similar to preindustrial values across the southern portion of our model domain (south of 40°S). With the imposed higher precipitation across the northern portion of the model domain, ice retreats slower during the last deglaciation relative to our standard simulation by >1 kyr, and in some locations up to 2 kyr."

We also will plan to add text to section 4.1 Ice-climate sensitivity, while removing the text concerning the PMIP4 simulations. This is in addition to the added text described in RC 2a above:

"Much of the TraCE-21ka simulated winter precipitation anomalies shown in Figure 9 are within 10% of the preindustrial value. The sensitivity tests conducted here suggest that modest changes (~10%) in precipitation can alter the pace of ice retreat across the CLD on timescales consistent with the resolution of geochronological proxies constraining past ice retreat. We note that while TraCE-21ka simulates variations in the precipitation across our model domain that are consistent with hydroclimate proxies discussed above (Moreno et al., 1999; 2015; 2018), the changes are not as large as proxy data across the CLD indicate. For example, hydroclimate proxies suggest that the LGM and early deglaciation was up to 2 times wetter across the CLD than present day (Moreno et al., 1999; Heusser et al., 1999). Therefore, we can deduct from our sensitivity analysis here that higher precipitation anomalies during the LGM and last deglaciation, forced by proposed changes in the SWW (Moreno et al., 1999;2015), may have helped offset melt from deglacial warming thereby influencing the pacing of early deglacial ice retreat in this region."

- Specific suggestions:

    - Figure 6 takes too much space for the content it presents.

      This has been removed as we have taken out the section using PMIP models.

- Line 428 & similar instances: Provide coordinates of these locations. Most people would not know where to look for them.

We have added locations to the Map (figure 2).

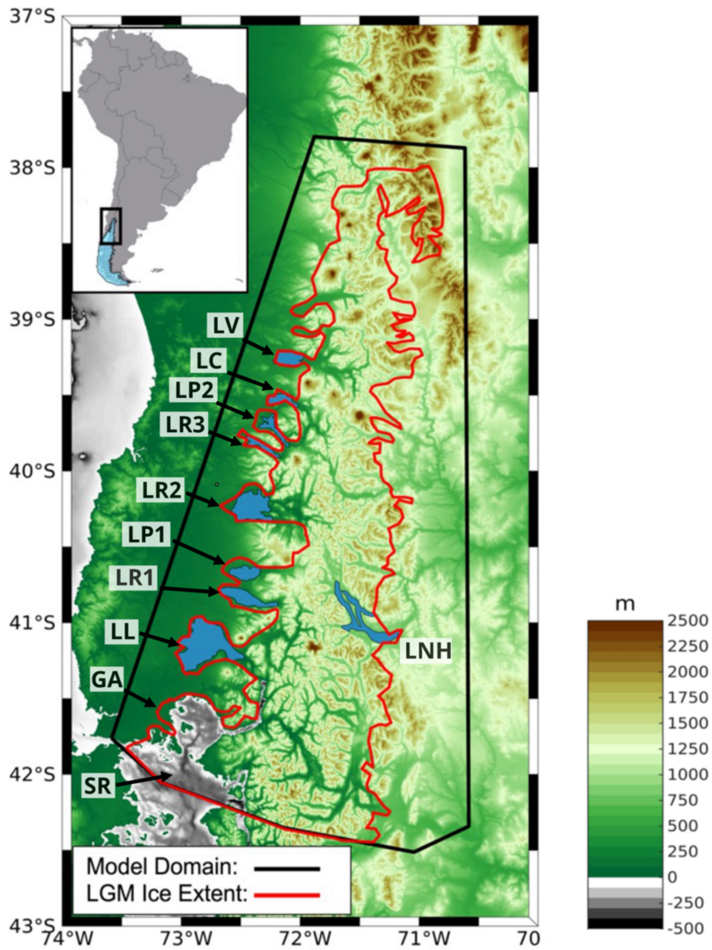

Figure 1. Bedrock topography for our study area (meters). Our model domain (shown as the black line), encompasses the reconstructed LGM ice limit (shown in red) from PATICE (Davies et al., 2020). Present day lakes are shown in blue, with abbreviated names as: SR (Seno de Reloncaví), GA (Golfo de Ancud), LL (**Lago Llanquihue), LR1 (Lago Rupanco)**, LP1 (Lago Puyehue), LR2 (Lago Ranco), LR3 (Lago Riñihue), LP2 (Lago Panguipulli), LC (Lago Calafquén), LV (Lago Villarica), LNH (Lago Nahuel Huapi).

- Figure 11: Missing the ice area from PATICE for 10 ka?

  We have added the area from the PATICE reconstruction for the 10 ka interval to the plot (figure 11).

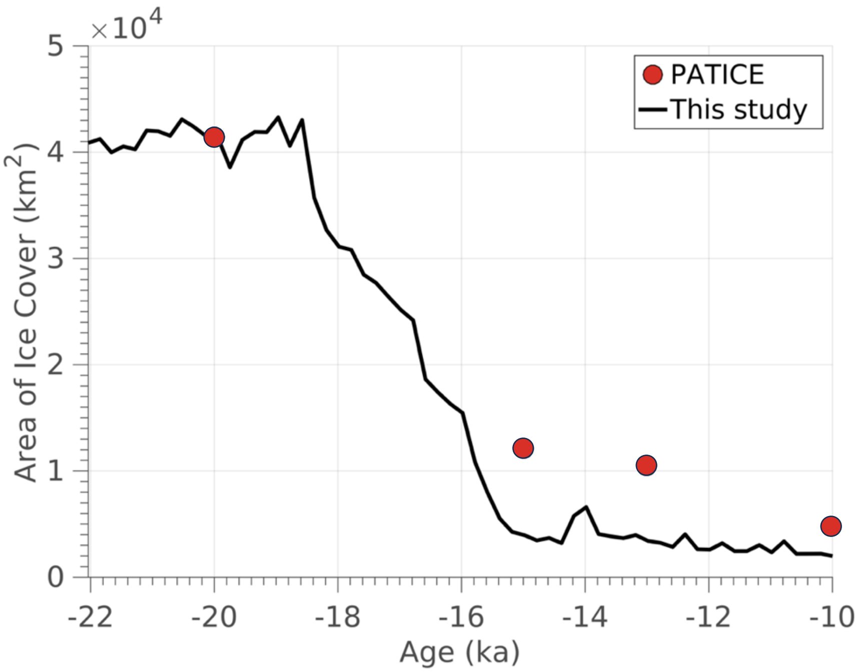

Figure 2. The simulated ice area (km^2) from 22 ka to 10 ka shown as the black line. The red dots indicate the calculated ice area across our model domain for the reconstructed ice extent from PATICE (Davies et al., 2020).

- Conclusions present some departures from the statistics found in the results and discussion. Could these be refined?

We have updated the Conclusions below:

"In this study, we use a numerical ice sheet model to simulate the LGM and deglacial ice history across the northernmost extent of the PIS, the CLD. The ice sheet model relied on inputs of temperature and precipitation from the TraCE-21ka climate model simulation covering the last 22,000 years in order to simulate the deglaciation of the PIS across the CLD into the early Holocene.

Our numerical simulation suggests that large scale ice retreat occurs after 19 ka coincident with rapid deglacial warming, with the northern portion of the CLD becoming ice free by 17 ka. The simulated ice retreat agrees well with the most comprehensive geologic assessment of past PIS history available (PATICE; Davies et al., 2020) for the LGM ice extent and early deglacial but diverge when considering the ice geometry at and after 15 ka. In our simulations, the PIS persists until 15 ka across the remainder of the CLD, followed by ice retreat to higher elevations as mountain glaciers and small ice caps persist into the early Holocene (e.g., Cerro Tronador). The geologic reconstruction from PATICE instead estimates a small ice cap persisting across the southern portion of high terrain in the CLD until about 10 ka. However, because there are limited geologic constraints particularly after 15 ka, high uncertainty in the timing and extent of deglacial ice history remains in the geologic reconstruction. Therefore, our results provide an additional reconstruction of the deglaciation of the PIS across the CLD that differs from PATICE after 15 ka, emphasizing a need for future work that aims to improve geologic reconstructions of past ice margin migration particularly during the later deglaciation across this region.

While deglacial warming was a primary driver of the demise of the PIS across the last deglaciation, we find that precipitation modulates the pacing and magnitude of deglacial ice retreat across the CLD. Paleoclimate proxies within the CLD has shown that the strength and position of the SWW varied during the LGM and last deglaciation, altering hydrologic patterns and influencing the deglacial mass balance. We find that the simulated changes in the strength and position of the SWW in TraCE-21ka are similar to those inferred by paleoclimate proxies of precipitation, consistent with a wetter than preindustrial climate being simulated and reconstructed over the CLD and in particular the region north of 40°S. Through a series of sensitivity tests, we alter the magnitude of the precipitation anomaly modestly (up to 10%) during our transient deglacial simulations and find that the pacing of ice retreat can speed up or slow down by a few hundred years and up to 2000 years depending on whether we impose an increase or decrease in the precipitation anomaly. While paleoclimate proxies of precipitation suggest that the CLD may have experienced twice as much precipitation during the LGM and early deglacial relative to present day (Moreno et al., 1999;2015), TraCE-21ka simulates smaller increases in LGM and early deglacial precipitation (~10-15% greater than preindustrial). Therefore, while our modelling suggests that modest changes in precipitation can modulate the pace of deglacial ice retreat across the CLD, from our analysis we can deduct that larger anomalies in precipitation as found in the paleoclimate proxies may have an even larger impact on modulating deglacial ice retreat. Because paleoclimate proxies of past precipitation are often lacking, and climate models can simulate a range of possible LGM and deglacial hydrologic states, these results suggest that improved knowledge of the past precipitation is critical towards better understanding the drivers of PIS growth and demise, especially as small variations in precipitation can modulate ice sheet history on scales consistent with geologic proxies."

JJA 925 hPA zonal wind

Figure S3 A-E. First column: The difference in the JJA 925 hPa zonal wind for each corresponding time period relative to the PI (in m/s). Positive values indicate increased zonal wind speed and negative values indicate decreased zonal wind speed relative to the PI. The magenta line is the position of the maximum zonal wind during the PI. The black line is the position of the maximum zonal wind for the corresponding time period. The red polygon denotes the location of our model domain. Second column: Zonal mean JJA 925 hPa wind (in m/s) averaged over -85 to -55 degrees west longitude for the PI and the corresponding time period. The time periods listed are computed over 500 yr periods (***LGM***: 22ka-21.5ka; ***18ka***: 18.5ka-18ka; ***16ka***: 16.5ka-16ka;

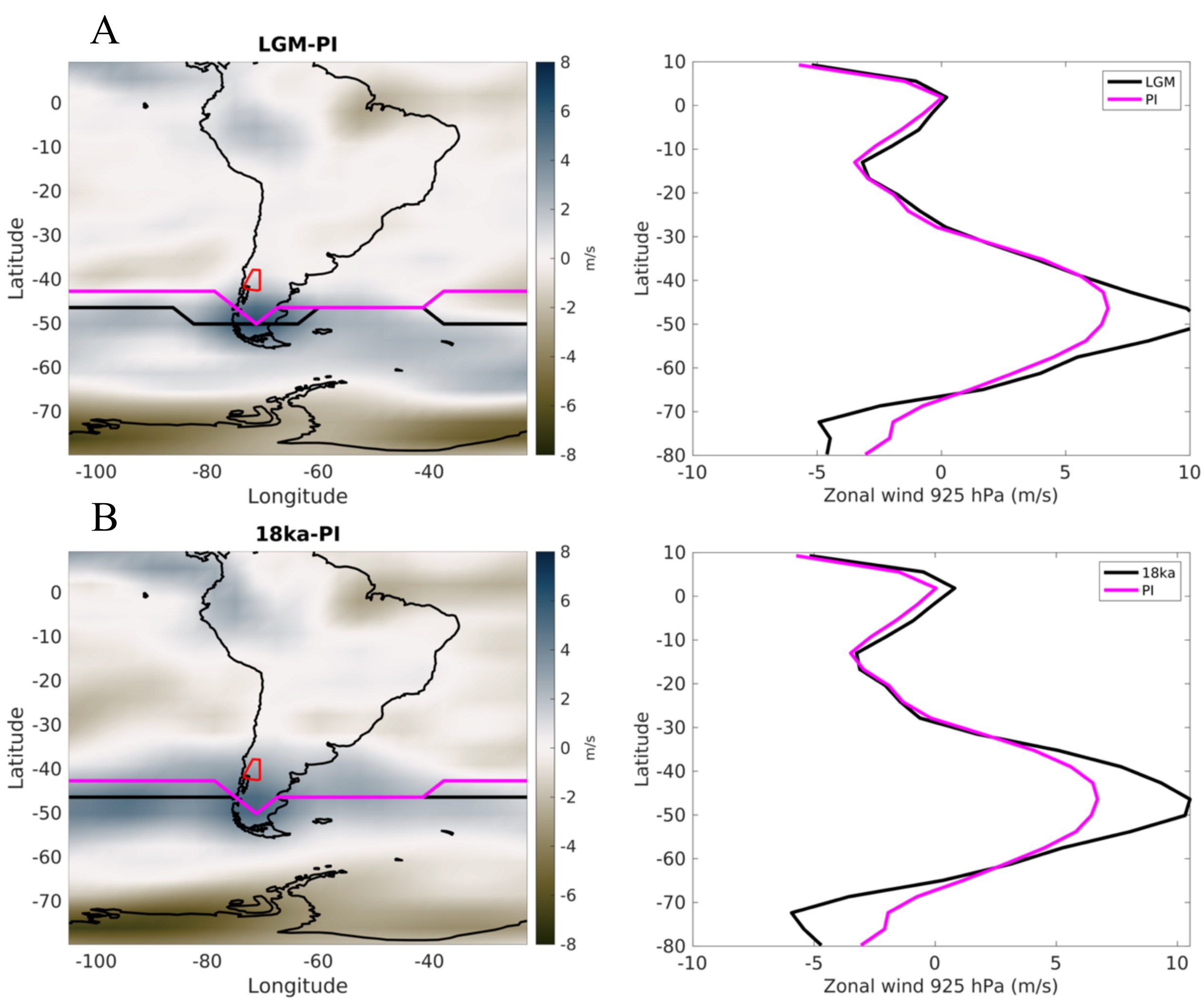

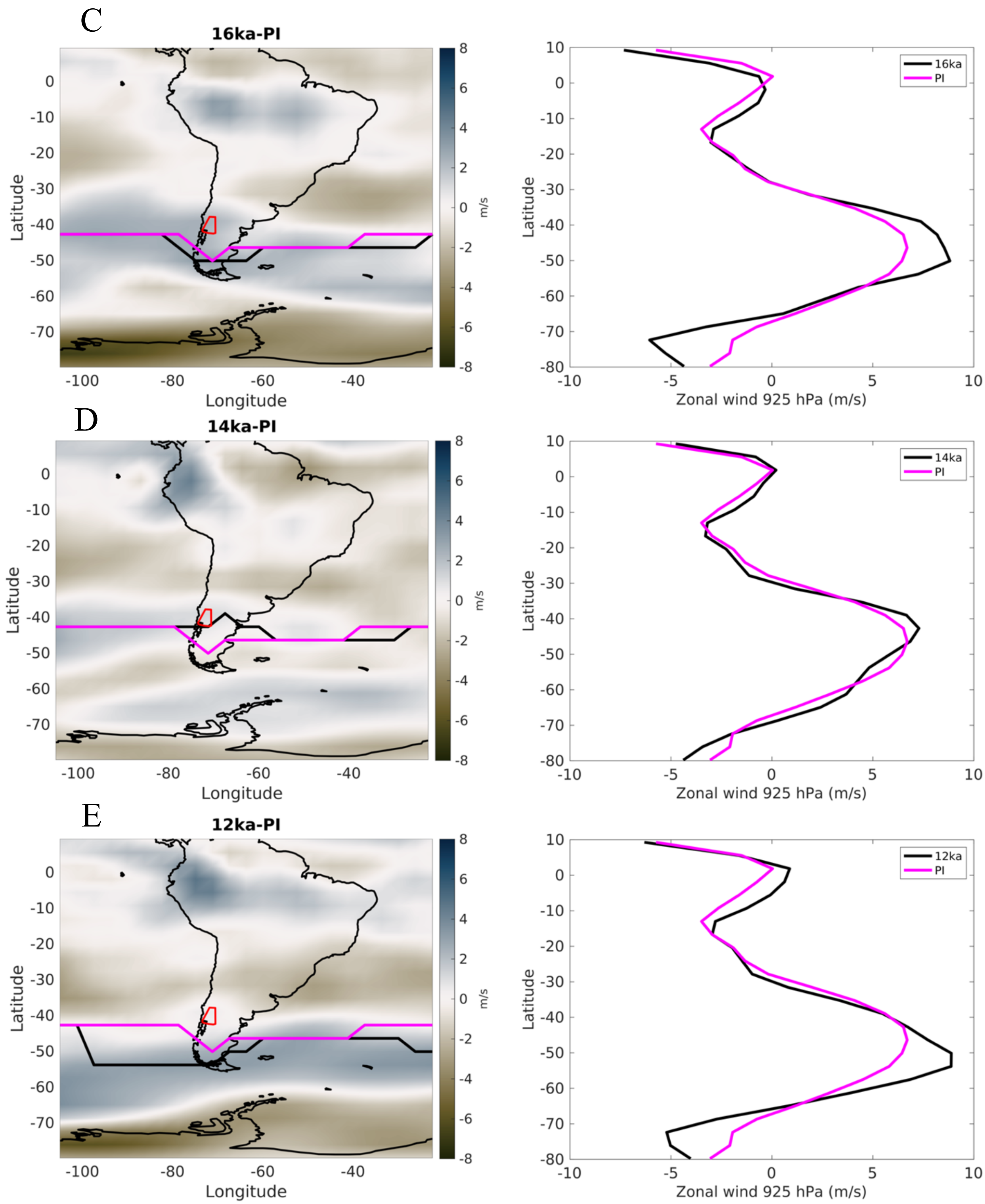
C
16ka-PI
Latitude
Longitude
m/s
16ka
PI
Zonal wind 925 hPa (m/s)
D
14ka-PI
Latitude
Longitude
m/s
14ka
PI
Zonal wind 925 hPa (m/s)
E
12ka-PI
Latitude
Longitude
m/s
12ka
PI
Zonal wind 925 hPa (m/s)

850 hPa Moisture Flux Convergence

We calculate the moisture flux convergence (MFC) at 850 hPa as:

$$-1(\nabla \cdot Vq)$$

where ∇ is the gradient operator, V is the horizontal wind vector (u,v), and q is the specific humidity. The divergence is multiplied in this case by -1 to show moisture flux convergence. We calculate the MFC at the ***LGM*** (22ka-21.5ka), ***18ka*** (18.5ka-18ka), ***16ka*** (16.5ka-16ka), ***14ka*** (14.5ka-14ka), and ***12ka*** (12.5ka-12ka) and then compute the difference at these periods against the **PI** (shown below in Figure S4A-E).

Figure S4 A-E. JJA moisture flux convergence at 850 hPA for each corresponding time period, computed as the difference from the PI (in g kg^{-1}s^{-1}). Positive anomalies indicate areas of greater moisture flux convergence relative to the PI and negative values indicate areas of greater moisture flux divergence relative to the PI. The wind vectors correspond to the anomaly relative to the PI for the 850 hPa pressure level. The red polygon denotes the location of our model domain. The time periods listed are computed over 500 yr periods (***LGM***: 22ka-21.5ka; ***18ka***: 18.5ka-18ka; ***16ka***: 16.5ka-16ka; ***14ka***: 14.5ka-14ka; ***12ka***: 12.5ka-12ka).

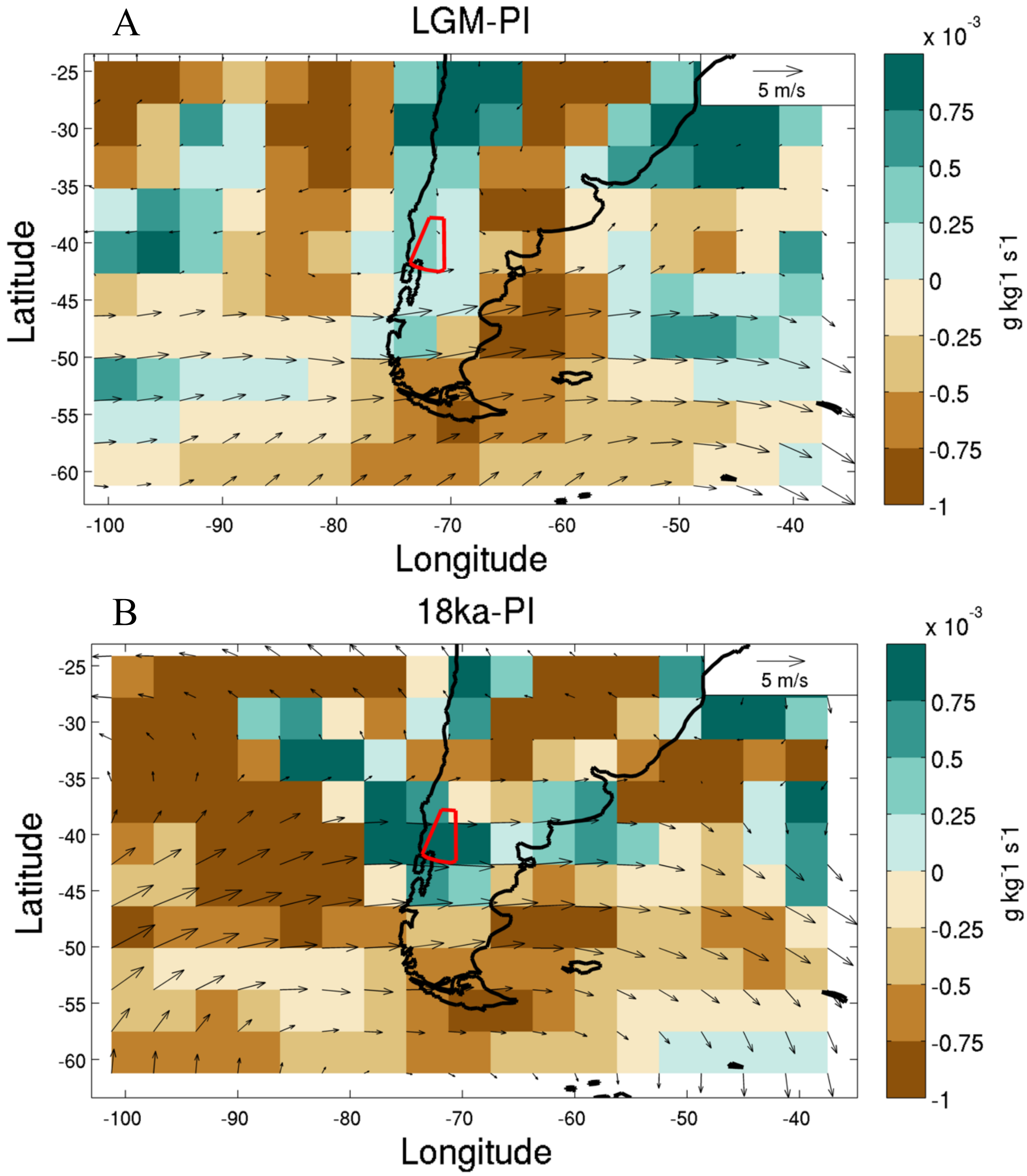

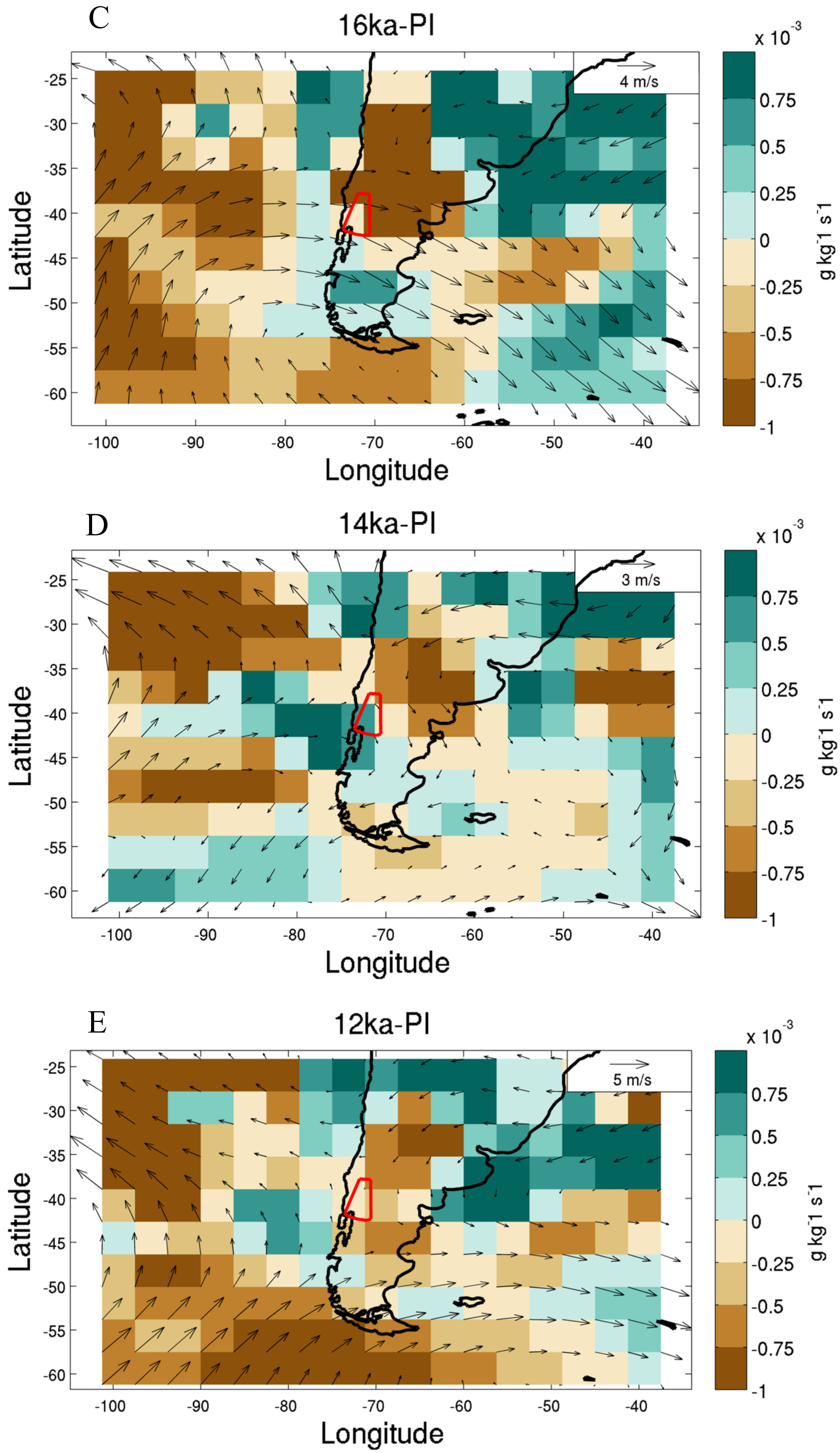

C
16ka-PI
4 m/s
x 10^-3
0.75
0.5
0.25
0
-0.25
-0.5
-0.75
-1
g kg-1 s-1
Latitude
-25
-30
-35
-40
-45
-50
-55
-60
-100
-90
-80
-70
-60
-50
-40
Longitude
D
14ka-PI
3 m/s
x 10^-3
0.75
0.5
0.25
0
-0.25
-0.5
-0.75
-1
g kg-1 s-1
Latitude
-25
-30
-35
-40
-45
-50
-55
-60
-100
-90
-80
-70
-60
-50
-40
Longitude
E
12ka-PI
5 m/s
x 10^-3
0.75
0.5
0.25
0
-0.25
-0.5
-0.75
-1
g kg-1 s-1
Latitude
-25
-30
-35
-40
-45
-50
-55
-60
-100
-90
-80
-70
-60
-50
-40
Longitude